LARGE-SIGNAL KLYSTRON SIMULATIONS USING KLSC

Bruce E. Carlsten, Los Alamos National Laboratory, Los Alamos, NM 87545 USA and

Patrick Ferguson, MDS Company, Oakland, CA 94611 USA

Abstract

We describe large-signal klystron simulations using the particle-in-cell code KLSC. This code uses the induced-current model to describe the steady-state cavity modulations and resulting rf fields, and advances the space-charge fields through Maxwell's equations. In this paper, an eight-cavity, high-power S-band klystron simulation is used to highlight various aspects of this simulation technique. In particular, there are specific issues associated with modeling the input cavity, the gain circuit, and the large-signal circuit (including the output cavities), that have to be treated carefully.

1 INTRODUCTION

We have recently developed a new large-signal klystron simulation code, KLSC. KLSC is a particle-in-cell code, and represents a significant advance over previously available simulation tools [1,2], which tended to use point-by-point space-charge forces, and were thus limited to less than a hundred simulation particles. In addition to the limitation on the number of particles, these codes also assumed that the space-charge fields could be solved electrostatically in some beam frame of reference, which is certainly not true when the beam is in the output cavity and there is a large energy spread. KLSC uses a uniform, rectangular mesh to calculate the space-charge fields, and advances the fields according to the Maxwell curl equations [3]. Particles travel along this mesh, being pushed by the Lorentz force equation. A charge-conserving algorithm is used to evolve the space-charge fields, where the current is determined from the particles' motion on the mesh. The cavity rf fields are superimposed on this mesh (the field distribution is provided by the code SUPERFISH), and superposition of both the space-charge and rf fields is used to determine the particle motion. This separation of the rf and space-charge fields is allowable; the only approximation that arises is that the boundary condition on the space-charge mesh does not include the cavity gaps and shapes around the cavity noses. The particle motion is used to calculate the driven modulation of the rf cavities. An iteration scheme is then used to converge on an rf field amplitude that leads to a self-consistent particle motion.

There are three separate regimes of large-signal klystron simulation, each with distinct simulation issues. These are the input cavity, the gain circuit (the cavities providing the gain from the small-signal amplitude in the input cavity to the large-signal amplitude in the penultimate and output cavities), and the large-signal circuit (the penultimate and output cavities).

TABLE 1: Operating Parameters

Operating frequency	3 GHz
Beam current	796 A
Beam voltage	720 kV
Input power	3.5 watt
Output power	310 MW
Efficiency	54%

The difficulties in the input cavity and the gain circuit are due to numerical stability of the iteration procedure. The iteration scheme is more straightforward for the large-signal circuit, and the issue here is the self-consistent simulation of multiple coupled output cavities.

In the next section, we will describe the induced current model used as a basis for the self-consistent calculation of the rf cavity field amplitudes, and the iteration schemes available for determining the self-consistent parameters. Following that, we will use a simulation of a high-power, S-band klystron, designed by MDS Company, to describe features of the simulation technique. First, we will present the model describing the input cavity's interaction with both the external drive and the electron beam, including the required input power as a function of input cavity loaded and unloaded Q and resonant frequency. Then, we will describe the calculation of the gain circuit, comparing the cavity modulation to that predicted by using the beam impedance in parallel to the cavity impedance. Finally, we will demonstrate the code's ability to handle multiple penultimate and output cavities, with three penultimate and two coupled output cavities. The nominal beam and cavity parameters are shown in Tables 1 and 2.

TABLE 2: Cavity Parameters

Cavity	Resonant Frequency	Shunt Impedance	R/Q	Voltage
1	3015 MHz	351 kΩ	124 Ω	709.3 V
2	2991	351	117	18.4 kV
3	3009	351	115	195
4	3330	432	144	182
5	3350	435	145	265
6	3420	450	150	310
7				894
8				1211

The first cavity is the input cavity. Cavities two and three are for gain and constitute the gain circuit. Cavities four through six are penultimate cavities, and, along with cavities seven and eight (the output cavities), make up the output circuit. Cavities seven and eight are coupled, with impedances $Z_{77} = (14.1 + j569)$ Ω, $Z_{78} = Z_{87} = (175 - j5.3)$ Ω, and $Z_{88} = (2315 - j67.2)$ Ω.

2 CAVITY/BEAM-INTERACTION MODEL

In Fig. 1 we see the circuit model for a cavity. The cavity impedance, Z_{cav}, is given in terms of the cavity shunt impedance R, the cavity resonant frequency f_0, the operating frequency f, and the cavity R/Q factor by

$$\frac{1}{Z_{cav}} = \frac{1}{R} + j\left(\frac{f}{f_0} - \frac{f_0}{f}\right)\frac{1}{R/Q} \quad .$$

There can also be some coupling to an external drive, which is not shown. The gap voltage is given by

$$V_{gap} = Z_{cav}i_1 \quad ,$$

where i_1 is the current in the cavity circuit due to the beam, usually known as the fundamental component of the beam induced current. The instantaneous induced current $i_{ind}(t)$ is given by Ramo's theorem [4],

$$i_{ind}(t) = \frac{\int_V \vec{J}(t)\cdot\vec{E}(t)\,dV}{V_{gap}(t)} \quad ,$$

where the space-charge current is given by $\vec{J}$, the electric field $\vec{E}$ is only from the cavity rf fields, and the integral is taken over the entire cavity volume V. The fundamental component of the induced current is defined by the expansion

$$i_{ind}(t) = i_0 + i_1\cos(\omega t + \phi_1) + i_2\cos(2\omega t + \phi_2) + \ldots$$

This set of equations (along with the Lorentz force equation for the particle motion due to the rf cavity fields) fully represent the self-consistent solution to the cavity excitation. The iteration scheme in KLSC is based on guessing a cavity voltage, pushing the electrons for an rf period, evaluating the fundamental component of the induced current, and re-evaluating the cavity voltage. If the re-evaluated cavity voltage is sufficiently close to the guess, the solution is considered to be self-consistent. If not, this procedure is iterated, typically using a weighted average of the newly calculated cavity voltage and the original guess as the guess for the next iteration, until a self-consistent solution is reached. The weighting factor is called the relaxation factor.
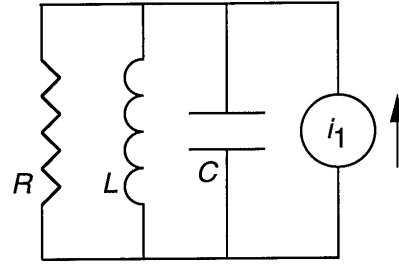

Figure 1. Beam/cavity interaction circuit

3 INPUT CAVITY

For the input cavity, we wish to calculate the input power drive required to establish a certain field amplitude. We could use the iterative procedure outlined above to find the effect of the induced current in the input cavity, but it does not typically converge (because the induced current counters nearly all of the input drive and thus small errors in the cavity voltage guess will lead to very large fluctuations in the re-evaluated cavity voltage). However, the procedure to find a self-consistent solution is straightforward for this cavity. The effect of the induced current is to establish an effective beam impedance, Z_{beam}, which acts in parallel with the cavity impedance. This beam impedance can be found by numerically calculating the induced current for a given cavity modulation - the induced current only depends on the cavity modulation and not on the cavity impedance itself. The beam impedance is then given by the cavity voltage divided by the fundamental component of the induced current [5]. The power required from the generator is

$$P_{in} = \frac{1}{8}|1+\beta|^2\frac{|V_{gap}|^2}{|Z_{cav}\|\beta|}\left|1 - \frac{Z_{cav}}{(1+\beta)Z_{beam}}\right|^2 \quad ,$$

where the cavity-input waveguide coupling is given by $\beta = Z_0 Z_{cav}/(2\pi f)^2 M^2$, and where Z_0 is the input waveguide characteristic impedance and M is the mutual inductance between the waveguide and the cavity. The cavity Q loaded by the input waveguide is given in terms by the coupling and the unloaded cavity Q, Q_0, by

$Q_l = Q_0 \dfrac{1}{1+\mathrm{Re}(\beta)}$. If the cavity is matched (no reflected power), the power from the generator is given by

$$P_{in} = \frac{1}{2}|V_{gap}|^2\left|\frac{Z_{cav} - Z_{beam}}{Z_{cav}Z_{beam}}\right| \quad .$$

The input is matched if the cavity detuning is

$$\frac{f_0 - f}{f} = -\frac{R/Q}{2}\mathrm{Im}(1/Z_{beam})$$

and the externally loaded cavity Q is

$$Q_l = Q_0 \frac{1}{1 + \text{Re}\left(\dfrac{Z_{beam} - Z_{cav}}{Z_{beam}}\right)} \quad .$$

4 GAIN CIRCUIT

The relaxation iteration scheme outlined in Section 2 also does not work well for the high gain cavities, for the same reason as for the input cavity. However, we cannot now simply use the beam impedance in parallel with the cavity impedance to find the cavity modulation - the cavity modulation directly affects the current modulation driving the cavity. For this case, the particles' motion must be simulated through the cavity and the induced current calculated. Instead of using relaxation to determine a new guess for the cavity voltage, the derivatives of the voltage equal to the induced current times the cavity impedance with respect to both the real and imaginary part of the guess voltage is found, and a new voltage is predicted. This two-dimensional Newton-Raphson approach is needed because the function defined by the induced current times the cavity impedance is not analytic.

The resulting self-consistent cavity voltage is somewhat different than would be found by simply assuming that the cavity and beam impedances were driven by the input current modulation. For the second cavity in this example, the self-consistent voltage is 18.35 kV, with a phase of 2.73 radians. Using the simple beam impedance approximation (and the induced current in the second cavity due only to the fields in the first cavity), one would have guessed that the cavity voltage should be 22.6 kV, with a phase of 2.96 radians. The error in the magnitude is from correlations between the induced current arising from the two cavities, and the error in phase is from the fact that there is no external drive power and the power in the cavity must come from the beam itself.

5 OUTPUT CIRCUIT

The output circuit, defined by the penultimate and output cavities, is comparatively simple to simulate. The relaxation iteration scheme works well for these cavities (the induced current is not drastically modified by the fields within the cavities themselves).

In Fig. 2, we plot the axial electric field at the center of the beam as a function of time at an axial location roughly between the output cavities. We see the axial field has reached steady-state after about 40 rf cycles, and that the higher harmonic fields are slipping in phase relative to the fundamental, due to the relatively large beam pipe. In Fig. 3, we plot the instantaneous current as a function of time at the same axial location. The beam is clearly well-bunched (the induced current in the output cavities is about 80% of the average beam current). The

gentle exponential rise of the current is also evident at the beginning of the plot. In Fig. 4, we plot the particles' $\gamma\beta_z$ as a function of axial position, at the end of the simulation. For this simulation, the first output cavity is centered at 1.1 m and the second at 1.14 m. The bunching and energy extraction is clear in this plot.
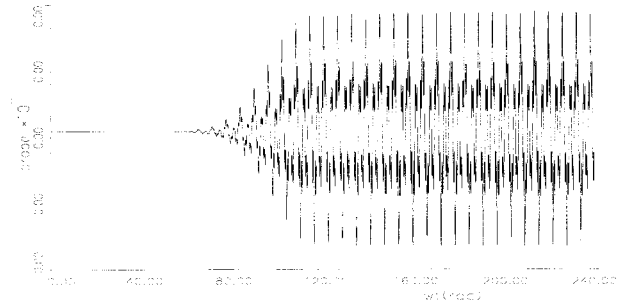

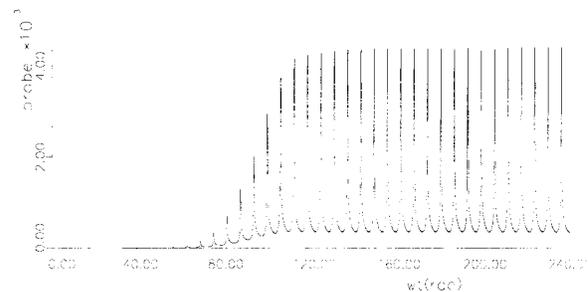Figure 2. Axial electric field versus time in the output circuit.

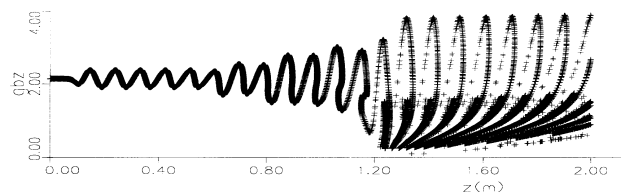Figure 3. Current modulation versus time in the output circuit.

Figure 4. Particle $\gamma\beta_z$ versus axial position at the end of the simulation.

REFERENCES

[1] H. Yonezawa and Y. Okazaki, "A one-dimensional disk model simulation for klystron design," SLAC technical note SLAC-TN-84-5 (1984).

[2] B. E. Carlsten, "A self-consisten numerical analysis of klystrons using large-signal beam-wave interaction simulations," PhD Thesis, Stanford University, Stanford (1985).

[3] C. K. Birdsall and A. B. Langdon, Plasma physics via computer simulations, McGraw-Hill Book Company, New York (1985).

[4] J. W. Gewartowski and H. A. Watson, Principles of electron tubes, Van Nostrand, New York (1965).

[5] B. E. Carlsten and P. Ferguson, "Numerical determination of the matching conditions and drive characteristics for a klystron input cavity with beam," IEEE Trans. Elec. Dev., **44**, 894 (1997).